Oxygen and Ruthenium Methylation of $Ru_2[(H_3C)_2PCH_2P(CH_3)_2]_2(CO)_5$. Formation and Interconversion of Terminal and Bridging Acetyl Ligands and Molecular Structure of $[Ru_2[(H_3C)_2PCH_2P(CH_3)_2]_2(\mu\text{-}COCH_3)(CO)_4][CF_3SO_3]$

Kimberly A. Johnson and Wayne L. Gladfelter*

Department of Chemistry, University of Minnesota, Minneapolis, Minnesota 55455

Received January 12, 1990

The reaction of $Ru_2(dmpm)_2(CO)_5$, where dmpm = bis(dimethylphosphino)methane, with methyl triflate ($CF_3SO_3CH_3$) results in the formation of two major products, which can be isolated by fractional crystallization. One product, obtained in 33% yield, results from methylation of the oxygen of the bridging carbonyl and contains a μ-methoxymethylidyne ligand. The structure of this compound has been determined by single-crystal X-ray crystallography (orthorhombic crystal system, *Pbca* space group, a = 15.325 (5) Å, b = 18.52 (1) Å, c = 20.324 (6) Å, V = 5769 (7) Å^3, Z = 8). The other product, isolated in 45% yield, was formulated as $[Ru_2(dmpm)_2(CO)_5(CH_3)][CF_3SO_3]$ on the basis of the mass spectrum and elemental analytical data. NMR spectroscopy shows that this complex contains a methyl group bonded directly to one Ru trans to the Ru–Ru bond. $[Ru_2(dmpm)_2(CO)_5(CH_3)][CF_3SO_3]$ was found to undergo subsequent migratory insertion to generate $[Ru_2(dmpm)_2(CO)_5[C(O)CH_3]]^+$ and $[Ru_2(dmpm)_2(CO)_4[\mu\text{-}C(O)CH_3]]^+$. The former has a ν_{CO} band at 1604 cm^{-1}, consistent with a terminal acetyl ligand, while the latter has ν_{CO} band at 1413 cm^{-1}, similar to that for other bridging acetyl ligands. Under a CO atmosphere, the terminal acetyl is formed exclusively. The terminal acetyl can then be converted to the bridging acetyl by simply stirring the solution under nitrogen.

Introduction

Binuclear, zerovalent ruthenium complexes having the structure shown in 1 are known for diphosphine (R = Ph, Me; Y = CH_2)[1,2] and diphosphazane ligands (R = OEt; Y = NEt).[3] Compared to the extensive studies[4-6] of the

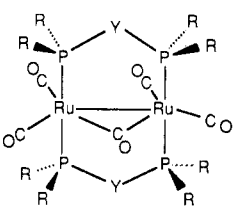

1

related A-frame complexes of other d^8 transition metals, very little is known about the reactivity of the ruthenium(0) binuclear complexes. We have been especially interested in exploring the chemistry of the electron-rich dimer $Ru_2(dmpm)_2(CO)_5$, where dmpm = bis(dimethylphosphino)methane, which can be easily prepared on a multigram scale by the reaction of $Ru_3(CO)_{12}$ with dmpm under high pressures of CO.[2] In this paper we describe the results from the methylation of $Ru_2(dmpm)_2(CO)_5$.

Experimental Section

General Considerations. $Ru_3(CO)_{12}$ (Strem), bis(dimethylphosphino)methane (dmpm, Strem), and methyl triflate (Aldrich) were used without further purification. $Ru_2(dmpm)_2(CO)_5$ was prepared as previously reported.[2] Carbon monoxide was used as received from Matheson. Toluene and diethyl ether (Et_2O) were dried by distillation from sodium benzophenone ketyl under nitrogen. Hexane was dried over sodium, and methylene chloride (CH_2Cl_2) was dried over calcium hydride. Both were distilled under N_2 prior to use. All reactions were conducted under a nitrogen atmosphere with use of standard Schlenk techniques. Infrared spectra were obtained on a Mattson Cygnus 25 FTIR spectrometer. ^{1}H NMR spectra were collected on an IBM AC-200 spectrometer, and ^{13}C NMR spectra were collected on an IBM AC-300 spectrometer. ^{31}P NMR spectra were recorded on a Nicolet NFT 300-MHz spectrometer. Elemental analyses were performed by M-H-W Laboratories. Table I contains a summary of the infrared and ^{1}H and ^{31}P NMR spectroscopic data. Simulations of complex ^{31}P NMR spectra were done with use of the program RACCOON written by Paul Schatz.

Reaction of $Ru_2(dmpm)_2(CO)_5$ with Methyl Triflate. $Ru_2(dmpm)_2(CO)_5$ (80 mg, 0.130 mmol) was charged to a 100-mL three-neck flask equipped with a stirbar, gas adapter, and pressure-equalizing addition funnel and then dissolved in CH_2Cl_2 (5 mL). $CF_3SO_3CH_3$ (15 μL, 0.130 mmol) was diluted in CH_2Cl_2 (6 mL) and then added dropwise over 10 min, and the yellow solution was stirred at room temperature for 1 h. The solution was condensed to half the original volume under vacuum; then Et_2O was added via syringe until the solution became cloudy. Yellow, feathery crystals, formulated as $[Ru_2(dmpm)_2(CO)_5(CH_3)][CF_3SO_3]$, were obtained from an approximately 1:1 mixture of CH_2Cl_2/Et_2O by slow cooling; yield 45 mg, 45%. ^{13}C NMR (CD_2Cl_2): δ −20.8 (s, CH_3), 16.8 (t, J_{CP} = 14.7 Hz, Me), 20.3 (t, J_{CP} = 16.3 Hz, Me), 47.5 (q, J_{CP} = 14.2 Hz, CH_2), 194.2 (mult, CO), 209.7 (t, J_{CP} = 12 Hz, CO), 211.6 (t, J_{CP} = 11 Hz, CO). Anal. Calcd for $[Ru_2(dmpm)_2(CO)_5(CH_3)][CF_3SO_3]$: C, 26.18; H, 3.98; P, 15.90. Found: C, 26.40; H, 4.16; P, 16.16. Mass spectrum (^{101}Ru): m/e 630, 63% relative intensity, $\{P\}^+$; fragments observed $\{P - nCO\}^+$, where n = 1–5. Further condensation of this solution and addition of Et_2O resulted in a crop of yellow, cubic crystals determined to be $[Ru_2(dmpm)_2(CO)_4(\mu\text{-}COCH_3)][CF_3SO_3]$, yield 33 mg, 33%. ^{13}C NMR (CD_2Cl_2): δ 18.8 (t, J_{CP} = 15.5 Hz, Me), 21.4 (t, J_{CP} = 18.5 Hz, Me), 37.1 (q, J_{CP} = 12.7 Hz, CH_2), 77.5 (s, OCH_3), 198.8 (mult, CO), 211.7 (mult, CO) 391.4 (mult, μ-$COCH_3$). Anal. Calcd for $[Ru_2(dmpm)_2(CO)_4(\mu\text{-}COCH_3)][CF_3SO_3]$: C, 26.18; H, 3.98; P, 15.90. Found: C, 25.67; H, 4.15; P, 15.41. Mass spectrum (^{101}Ru): m/e 630, 70% rel intensity, $\{P\}^+$; fragments observed $\{P - nCO\}^+$, where n = 1–4.

Carbonylation of $[Ru_2(dmpm)_2(CO)_5(CH_3)][CF_3SO_3]$. $[Ru_2(dmpm)_2(CO)_5(CH_3)][CF_3SO_3]$ (37.7 mg, 0.048 mmol) was

(1) Engel, D. W.; Moodley, K. G.; Subramony, L.; Haines, R. J. *J. Organomet. Chem.* **1988**, *349*, 393.
(2) Johnson, K. A.; Gladfelter, W. L. *Organometallics* **1989**, *8*, 2866.
(3) Leeuw, G. D.; Field, J. S.; Haines, R. J.; McCulloch, B.; Meintjies, E.; Monberg, C.; Olivier, G. M.; Ramdial, P.; Sampson, C. N.; Sigwarth, B.; Steen, N. D.; Moodley, K. G. *J. Organomet. Chem.* **1984**, *275*, 99.
(4) Balch, A. L. *ACS Symp. Ser.* **1981**, *No. 155*, 167.
(5) Puddephatt, R. J. *Chem. Soc. Rev.* **1983**, *12*, 99.
(6) Chaudret, B.; Delavaux, B.; Poilblanc, R. *Coord. Chem. Rev.* **1988**, *86*, 191.

0276-7333/90/2309-2101$02.50/0

Table I. Spectroscopic Data

compd[a]	ν_{CO}, cm^{-1}	^1H NMR,[b] ppm	^{31}P NMR,[c] ppm
$[Ru_2(dmpm)_2(\mu\text{-}COCH_3)(CO)_4]^+$	2012 m, 1974 s, 1946 m (CH_2Cl_2)	1.59 (s, Me), 1.62 (s, Me), 1.77 (mult, CH_2), 4.59 (s, OCH_3)	11.1 (s)
$[Ru_2(dmpm)_2(CH_3)(CO)_5]^+$	2013 m, 1971 s (CH_2Cl_2)	0.11 (t, J_{HP} = 5.4 Hz, Ru-Me), 1.56 (t, J_{HP} = 2.9 Hz, Me), 1.74 (t, J_{HP} = 3.1 Hz, Me), 2.73 (q, J_{HP} = 4.8 Hz, CH_2)	AA'BB'[d]
$[Ru_2(dmpm)_2[C(O)CH_3](CO)_5]^+$	2020 m, 1981 s, 1943 w, 1604 w (CH_2Cl_2)	1.68 (Me), 1.75 (t, J_{HP} = 3.2 Hz, Me), 2.54 (s, $C(O)CH_3$), 2.77 (q, J_{HP} = 4.8 Hz, CH_2)	AA'BB'[e]
$[Ru_2(dmpm)_2[\mu\text{-}C(O)CH_3](CO)_4]^+$	2018 m, 1985 s, 1957 m, 1413 w (CH_2Cl_2)	1.74 (t, J_{HP} = 3.3 Hz, Me), 1.85 (t, J_{HP} = 3.3 Hz, Me), 2.57 (s, $C(O)CH_3$), 2.65 (mult, CH_2)	−0.545 (t, J_{PP} = 42 Hz), 4.7 (t, J_{PP} = 42 Hz)

[a] All as triflate salts. [b] In CD_2Cl_2. [c] In CD_2Cl_2; relative to H_3PO_4. [d] δ_1 = 0.68 ppm, δ_2 = 1.80 ppm; J_{12} = 310 Hz, $J_{13} = J_{24}$ = 50 Hz, $J_{14} = J_{23}$ = 19 Hz, J_{34} = 295 Hz. [e] δ_1 = 0.25 ppm, δ_2 = 1.15 ppm; J_{12} = 302 Hz, $J_{13} = J_{24}$ = 50 Hz, $J_{14} = J_{23}$ = 19 Hz, J_{34} = 293 Hz.

Table II. Summary of Crystallographic Data

Crystal Parameters	
compd	$[Ru_2(dmpm)_2(CO)_4(\mu\text{-}COCH_3)][CF_3SO_3]$
cryst syst	orthorhombic
space group	*Pbca*
formula	$Ru_2C_{17}F_3H_{31}O_8P_4S$
fw	778.52
a, Å	15.325 (5)
b, Å	18.52 (1)
c, Å	20.324 (6)
V, Å^3	5769 (7)
Z	8
ρ(calcd), g cm^{-3}	1.79
temp, °C	−84 (1)
abs coeff, cm^{-1}	13.71
cryst dimens, mm	0.600 × 0.500 × 0.300
transmissn factors, max–min, %	119–90
abs cor applied	empirical (DIFABS)
Measurement of Intensity Data	
diffractometer	Enraf-Nonius CAD-4
radiation	Mo Kα (λ = 0.710 73 Å)
monochromator	graphite crystal
programs used	TEXSAN
method of structure soln	direct methods
scan type	ω–2θ
scan range, deg	0–49.9
rflns measd	*hkl*
no. of unique rflns	5232
no. of rflns used	3982
cutoff	3σ
p	0.05
extinction coeff	1.4385×10^{-8}
R	0.038
R_w	0.051
error in observn of unit wt	1.49

charged to a 50-mL three-neck flask equipped with a stirbar and gas adapter and then dissolved in CH_2Cl_2 (5 mL). The atmosphere of the flask was purged with CO at room temperature for 1 h, at which point the infrared spectrum of the solution indicated the reaction was complete. While the mixture was still under CO, hexane (3 mL) was added to the solution, causing pale yellow, plate-shaped crystals to form upon cooling. These crystals were air-stable but lost solvent; yield 25.5 mg, 65%. ^{13}C NMR (CD_2Cl_2): δ 17.76 (t, J_{CP} = 14.1 Hz, Me), 20.5 (t, J_{CP} = 16.5 Hz, Me), 48.69 (q, J_{CP} = 14.4 Hz, CH_2), 50.58 (s, $C(O)CH_3$), 190.7 (mult, CO), 207.7 (t, J_{CP} = 14 Hz, CO), 213 (t, J_{CP} = 13 Hz, CO), 247.8 (mult, $C(O)CH_3$). Anal. Calcd for $[Ru_2(dmpm)_2(CO)_5[C(O)CH_3]][CF_3SO_3]$: C, 26.76; H, 3.84; P, 15.35. Found: C, 26.81; H, 4.00; P, 15.41. Mass spectrum (^{101}Ru): *m/e* 658, 15% relative intensity $\{P\}^+$; fragments observed $\{P - nCO\}^+$, where *n* = 1–5. When a solution of this material was stirred 24 h at room temperature under N_2, the IR spectrum showed complete reaction to form another product in 92% yield. ^{13}C NMR (CD_2Cl_2): δ 17.4 (t, J_{CP} = 15.3 Hz, Me), 20.3 (t, J_{CP} = 15.8 Hz, Me), 41.8 (q, J_{CP} = 12 Hz, CH_2), 51.8 (s, $C(O)CH_3$), 208.5 (mult, CO), 208.7 (mult CO), 209.8 (mult, CO) 210.9 (mult, CO), 293.8 (mult, $C(O)CH_3$). Anal. Calcd for $[Ru_2(dmpm)_2(CO)_4[\mu\text{-}C(O)CH_3]][CF_3SO_3]$: C, 26.18; H, 3.98; P, 15.90. Found: C, 26.34; H, 4.18; P, 15.77. Mass spectrum (^{101}Ru): *m/e* 630, 75% rel intensity $\{P\}^+$; fragments observed $\{P - nCO\}^+$, where *n* = 1–4.

Scheme I

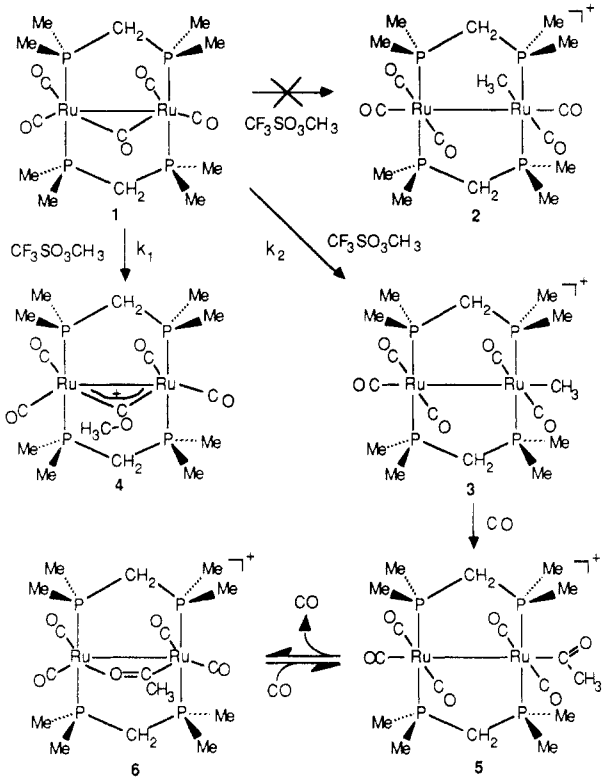

X-ray Crystallography of $[Ru_2(dmpm)_2(CO)_4(\mu\text{-}COCH_3)][CF_3SO_3]$. Yellow crystals were grown as described above. A suitable crystal was mounted on a fiber and cooled to −84 °C. Table II includes the details of the structural analysis. A preliminary peak search of 24 centered reflections (26° < 2θ < 42°) indicated that the crystal was orthorhombic. The space group was uniquely determined to be *Pbca* (No. 61) on the basis of the systematic absences (0*kl*, *k* = 2*n* + 1; *h*0*l*, *l* = 2*n* + 1; *hk*0, *h* = 2*n* + 1). During data collection, no decay of intensity was observed in three check reflections. All non-hydrogen atoms were refined anisotropically. Hydrogen atoms were included in the structure factor calculation in idealized positions with d_{C-H} = 0.95 Å and an isotropic temperature factor 20% greater than the B_{eq} of the carbon to which they were bonded. The maximum and minimum peaks on the final difference Fourier map corresponded to +1.62 and −0.82 e/Å^3, respectively. The values of the atomic scattering factors used in the calculations were taken from the usual tabulations,[7-9] and the effects for anomalous dispersion were

(7) Cromer, D. T.; Ibers, J. A. *International Tables for X-ray Crystallography*; Kynoch Press: Birmingham, England, 1974; Vol. IV, Table 2.2C.

Table III. Positional Parameters for $[Ru_2(dmpm)_2(CO)_4(\mu\text{-}COCH_3)][CF_3SO_3]$

atom	x	y	z
Ru1	0.65756 (3)	0.19700 (2)	0.60482 (2)
Ru2	0.53907 (3)	0.27918 (2)	0.68013 (2)
C1B	0.6682 (4)	0.2559 (3)	0.6873 (3)
O1B	0.7336 (3)	0.2722 (2)	0.7204 (2)
C13	0.7261 (5)	0.3246 (4)	0.7746 (4)
C11	0.5843 (4)	0.1758 (3)	0.5292 (3)
O11	0.5399 (3)	0.1660 (3)	0.4846 (2)
C12	0.7652 (4)	0.1504 (3)	0.5907 (3)
O12	0.8309 (3)	0.1218 (2)	0.5824 (2)
C21	0.5018 (4)	0.3431 (3)	0.7460 (3)
O21	0.4773 (4)	0.3818 (3)	0.7859 (3)
C22	0.4368 (4)	0.2563 (3)	0.6293 (3)
O22	0.3783 (3)	0.2409 (3)	0.5974 (3)
P11	0.71634 (9)	0.29719 (8)	0.55068 (7)
P12	0.6062 (1)	0.09213 (8)	0.65661 (9)
P21	0.5648 (1)	0.37790 (7)	0.60978 (8)
P22	0.5088 (1)	0.18420 (8)	0.75322 (8)
C1	0.6769 (4)	0.3834 (3)	0.5802 (3)
C2	0.5785 (4)	0.1060 (3)	0.7429 (3)
C3	0.6969 (4)	0.2994 (3)	0.4632 (3)
C4	0.8336 (4)	0.3095 (3)	0.5589 (4)
C5	0.4994 (4)	0.3827 (3)	0.5349 (3)
C6	0.5498 (4)	0.4676 (3)	0.6451 (4)
C7	0.5116 (5)	0.0503 (4)	0.6204 (4)
C8	0.6821 (5)	0.0172 (4)	0.6615 (4)
C9	0.3993 (4)	0.1480 (3)	0.7521 (3)
C10	0.5258 (5)	0.2049 (4)	0.8401 (3)
S1X	0.2068 (1)	0.01083 (9)	0.6225 (1)
O1X	0.1711 (3)	−0.0367 (3)	0.6725 (2)
O2X	0.2564 (4)	0.0688 (3)	0.6480 (3)
O3X	0.1468 (3)	0.0288 (3)	0.5712 (3)
C1X	0.2823 (5)	−0.0450 (4)	0.5802 (4)
F1X	0.3203 (4)	−0.0114 (3)	0.5304 (3)
F2X	0.3485 (3)	−0.0668 (3)	0.6209 (3)
F3X	0.2473 (3)	−0.1071 (2)	0.5599 (3)

Table IV. Cation Bond Distances (Å) in $[Ru_2(dmpm)_2(CO)_4(\mu\text{-}COCH_3)][CF_3SO_3]$

A. Metal–Metal and Metal–Ligand Distances			
Ru1–Ru2	2.821 (1)	Ru2–P21	2.354 (2)
Ru1–P11	2.338 (2)	Ru2–P22	2.349 (2)
Ru1–P12	2.345 (2)	Ru2–C21	1.876 (7)
Ru1–C11	1.944 (6)	Ru2–C22	1.924 (6)
Ru1–C12	1.884 (6)	Ru2–C1B	2.031 (6)
Ru1–C1B	2.006 (6)		
B. Intraligand Distances			
P11–C1	1.811 (6)	P21–C1	1.823 (6)
P12–C2	1.822 (7)	P22–C2	1.812 (6)
C11–O11	1.147 (7)	C21–O21	1.145 (8)
C12–O12	1.150 (7)	C22–O22	1.143 (7)
C1B–O1B	1.245 (7)		

included for the non-hydrogen atoms. The positional parameters, bond distances, and bond angles are listed in Tables III–V.

Results

As summarized in Scheme I, the reaction of $Ru_2(dmpm)_2(CO)_5$ with methyl triflate yields two products. On the basis of mass spectrometry and elemental analytical data, both products were formulated as $[Ru_2(dmpm)_2(CO)_5(CH_3)][CF_3SO_3]$. The ^1H NMR spectrum of the reaction mixture exhibited a singlet at 4.59 ppm, a chemical shift region characteristic of methoxy protons, suggesting that methylation occurred at the oxygen of one of the carbonyls. Also observed was a triplet at 0.1 ppm, indicating a methyl group was also bound to one of the metal centers. Two crystal morphologies were clearly present, which allowed a manual separation of the two pure compounds. Subsequently, we found that by carefully controlling the crystallization conditions, crops of crystals that were enriched in one or the other species could be obtained. The first crop of crystals from a given reaction were very fine needles. The ^1H NMR spectrum of these fine needles established that the major component was the Ru-methylated species $[Ru_2(dmpm)_2(CO)_5(CH_3)]^+$, with only a small amount of the μ-methoxymethylidyne complex $[Ru_2(dmpm)_2(CO)_4(\mu\text{-}COCH_3)]^+$ (**4**) present. Two possible structures for $[Ru_2(dmpm)_2(CO)_5(CH_3)]^+$ (**2** and **3**) were considered. The ^1H NMR spectrum exhibited two signals for the phosphine methyl groups and one quintet for the methylene protons, suggesting the methyl group of $[Ru_2(dmpm)_2(CO)_5(CH_3)]^+$ was bound in a symmetrical position (**3**). This structure makes the phosphine methyl groups on the Ru(1) end different from those on the Ru(2) end while rendering all four methylene protons equivalent. Also consistent with **3** is the ^{13}C NMR spectrum, which exhibits the metal-bound methyl signal at −20.8 ppm, and the carbonyl resonances at 211.6, 209.7, and 194.2 ppm occurred in a 2:2:1 intensity ratio. Finally, the ^{31}P NMR spectrum showed an AA′BB′ pattern consistent with **3**.

Subsequent crops of crystals from the same reaction were larger and more cube-shaped. The ^1H NMR spectrum of these crystals showed the major component to be the μ-methoxymethylidyne species (**4**). The two signals observed for the protons of the phosphine methyl groups and the singlet in the ^{31}P NMR spectrum reflect the high symmetry of this molecule. The two sets of multiplets due to the methylene protons revealed the μ-methoxymethylidyne ligand was bridging the metal centers on one face of the molecule.

The methylation of $Ru_2(dmpm)_2(CO)_5$ has been studied by low-temperature ^{31}P NMR spectroscopy. It was found that the signals due to the Ru-methylated product (**3**) and the O-methylated product (**4**) both appeared upon mixing at −90 °C and grew in at approximately the same rate as the reaction mixture was slowly warmed to room temperature. Long-term ^1H NMR studies have shown there is no interconversion of $[Ru_2(dmpm)_2(CO)_5(CH_3)]^+$ (**3**) and $[Ru_2(dmpm)_2(CO)_4(\mu\text{-}COCH_3)]^+$ (**4**), which discounts the existence of an equilibrium between the two species. The

Table V. Cation Bond Angles (deg) for $[Ru_2(dmpm)_2(CO)_4(\mu\text{-}COCH_3)][CF_3SO_3]$

A. Ligand–Metal–Ligand Angles			
C11–Ru1–C12	107.0 (2)	C22–Ru2–C21	105.9 (3)
C11–Ru1–C1B	144.8 (2)	C22–Ru2–C1B	141.8 (3)
C11–Ru1–P12	89.6 (2)	C22–Ru2–P22	90.8 (2)
C11–Ru1–P11	90.6 (2)	C22–Ru2–P21	88.9 (2)
C11–Ru1–Ru2	99.6 (2)	C22–Ru2–Ru1	96.6 (2)
C12–Ru1–C1B	107.8 (2)	C21–Ru2–C1B	112.3 (3)
C12–Ru1–P12	89.0 (2)	C21–Ru2–P22	87.8 (2)
C12–Ru1–P11	87.4 (2)	C21–Ru2–P21	89.7 (2)
C12–Ru1–Ru2	153.4 (2)	C21–Ru2–Ru1	157.5 (2)
C1B–Ru1–P12	95.9 (2)	C1B–Ru2–P22	89.3 (2)
C1B–Ru1–P11	86.0 (2)	C1B–Ru2–P21	92.6 (2)
C1B–Ru1–Ru2	46.0 (2)	C1B–Ru2–Ru1	45.3 (2)
P12–Ru1–P11	176.30 (5)	P22–Ru2–P21	177.26 (7)
P12–Ru1–Ru2	89.28 (5)	P22–Ru2–Ru1	93.78 (5)
P11–Ru1–Ru2	94.31 (5)	P21–Ru2–Ru1	88.96 (5)
B. Metal–Carbonyl and –Phosphine Angles			
Ru1–P11–C1	114.5 (2)	Ru2–P21–C1	113.7 (2)
Ru1–P12–C2	113.2 (2)	Ru2–P22–C2	114.1 (2)
Ru1–C11–O11	177.3 (5)	Ru2–C22–O22	177.0 (6)
Ru1–C12–O12	179.6 (5)	Ru2–C21–O21	178.6 (6)
Ru1–C1B–O1B	130.5 (4)	Ru2–C1B–O1B	140.5 (5)
P11–C1–P21	112.0 (3)	P12–C2–P22	111.2 (3)
Ru1–C1B–Ru2	88.7 (3)		

(8) Cromer, D. T.; Waber, J. T. *International Tables for X-ray Crystallography*; Kynoch Press: Birmingham, England, 1974; Vol. IV, Table 2.2A.

(9) Cromer, D. T. *International Tables for X-ray Crystallography*; Kynoch Press: Birmingham, England, 1974; Vol. IV, Table 2.3.1.

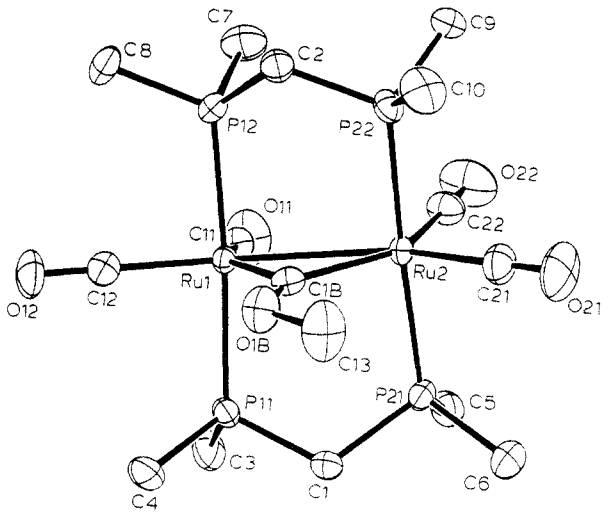

Figure 1. Structure of the cation of $Ru_2(dmpm)_2(CO)_4(\mu\text{-}COCH_3)][CF_3SO_3]$ showing the thermal ellipsoids at the 50% probability level.

photochemically induced conversion of $HRu_3(\mu\text{-}COCH_3)(CO)_{10}$ into $HRu_3[\mu\text{-}C(O)CH_3](CO)_{10}$ is the only known example of such a reaction.[10] The observation that the two products form at approximately the same rate suggests that there is no significant preference for attack at either the oxygen or the metal center.

Structure of $[Ru_2(dmpm)_2(CO)_4(\mu\text{-}COCH_3)][CF_3SO_3]$ ([4][CF_3SO_3]). Single-crystal X-ray crystallography of **4** showed the structure consists of well-separated anions and cations and, as shown in Figure 1, the connectivity is the same as that of the parent dimer $Ru_2(dmpm)_2(CO)_5$[2] with the additional methyl group bound to the oxygen of the bridging carbonyl. The carbonyls and the μ-methoxymethylidyne group define an equatorial plane surrounding the ruthenium atoms, and the phosphines occupy the axial positions. The angle between the planes comprised of Ru1–Ru2–C1B and Ru1–Ru2–P11–P12 is 80.63° and between Ru1–Ru2–C1B and Ru1–Ru2–P21–P22 is 94.73°. The Ru1–Ru2 bond length of 2.821 (1) Å is significantly shorter than that of the parent dimer $Ru_2(dmpm)_2(CO)_5$ (2.8928 (8) Å), and the Ru–C distances of the bridging methylidyne (2.006 (6) and 2.031 (6) Å) are shorter than the Ru–C bonds of the bridging carbonyl in $Ru_2(dmpm)_2(CO)_5$ (2.091 (4) and 2.114 (3) Å), which would be consistent with the delocalized multiple-bond character depicted in **4** (Scheme I). This constriction of the Ru–Ru distance placed enough strain on the fairly rigid dmpm bridges that it resulted in the twisting of the Ru_2P_4 framework, as evaluated by the angle between the two planes Ru1–Ru2–P11–P12 and Ru1–Ru2–P21–P22 of 14.10°. Apparently this is the first report of a structurally characterized binuclear μ-alkoxymethylidyne complex. It is, however, closely related to $[Ru_2Cp_2(CO)_3(\mu\text{-}CCH_3)][BF_4]$, which contains a bridging ethylidyne ligand.[11] The same pattern of equivalent Ru–C bond lengths supports the delocalized bonding description, although the Ru–Ru and both of the Ru–C (of the CCH_3 ligand) bonds were approximately 0.1 Å shorter than those found in $[Ru_2(dmpm)_2(CO)_4(\mu\text{-}COCH_3)][CF_3SO_3]$ ([4][CF_3SO_3]).

Carbonylation of $[Ru_2(dmpm)_2(CO)_5(CH_3)][CF_3SO_3]$ ([3][CF_3SO_3]). Stirring a solution of $[Ru_2(dmpm)_2(CO)_5(CH_3)][CF_3SO_3]$ under CO resulted in its carbonylation to yield a species formulated by mass spectrometry and elemental analysis as $[Ru_2(dmpm)_2(CO)_5[C(O)CH_3]][CF_3SO_3]$. The chemical shift of the methyl group in the ^1H NMR spectrum at 2.54 ppm and the band in the infrared spectrum at ν_{CO} = 1604 cm^{-1} were both consistent with a terminal acetyl ligand. The ^1H NMR spectrum also showed two triplets for the phosphine methyl groups and one quintet for the methylene protons, suggesting the acetyl ligand was bound in the same position as the methyl group in **3**. The signal in the ^{13}C NMR spectrum of this species at 248.7 ppm and the AA'BB' pattern in the ^{31}P NMR spectrum were consistent with this observation. On the basis of these spectroscopic data, we assigned the structure of $[Ru_2(dmpm)_2(CO)_5[C(O)CH_3]]^+$ as that shown in **5** (Scheme I).

Stirring a solution of **5** under N_2 at room temperature for 12–16 h resulted in loss of one CO ligand, as determined by the mass spectrum and elemental analysis. The chemical shift of the methyl group in the ^1H NMR spectrum at 2.57 ppm and the new band in the infrared spectrum at ν_{CO} = 1413 cm^{-1} suggested a rearrangement of the acetyl ligand to a bridging conformation (**6**). The energy of the ν_{CO} band of bridging acyl ligands in strongly dependent on the amount of oxycarbene character present[12] and ranges from 1339 (for $Cp_2ZrMo(Cp)[\mu\text{-}C(O)CH_3](CO)_2$[13]) to 1550 cm^{-1} (for $Ru_2[\mu\text{-}C(O)CH_3]_2(CO)_6$[14,15]). The shift of the acetyl carbon signal in the ^{13}C NMR spectrum from 247.8 to 293.8 ppm is consistent with a substantial increase of carbene character in the Ru–C interaction. When a solution of the μ-acetyl species **6** was stirred under CO, the terminal acetyl compound **5** was reformed. A summary of this reactivity is shown in Scheme I.

Discussion

Electrophilic alkylation of monometallic carbonyl complexes occurs at the metal;[16,17] however, alkylation of metal carbonyl clusters containing bridging CO ligands occurs at the carbonyl oxygen.[18] There are numerous examples of electrophilic alkylations of binuclear complexes containing bridging CO ligands that lead to O-alkylation[19,20] *or* M-alkylation.[21-23] $Ru_2(dmpm)_2(CO)_5$ is unusual in that its molecular and electronic structure allow it to react as an ambident nucleophile; alkylation occurs with equal

(10) Friedman, A. E.; Ford, P. C. *J. Am. Chem. Soc.* **1986**, *108*, 7851.
(11) Davies, D. L.; Dyke, A. F.; Endesfelder, A.; Knox, S. A. R.; Naish, P. J.; Orpen, A. G.; Plaas, D.; Taylor, G. E. *J. Organomet. Chem.* **1980**, *198*, C43.
(12) Rosen, R. P.; Hoke, J. B.; Whittle, R. R.; Goeffroy, G. L.; Hutchinson, J. P.; Zubieta, J. A. *Organometallics* **1984**, *3*, 846.
(13) Marsella, J. A.; Huffman, J. C.; Caulton, K. G.; Longato, B.; Norton, J. R. *J. Am. Chem. Soc.* **1982**, *104*, 6360.
(14) Kampe, C. E.; Boag, N. M.; Kaesz, H. D. *J. Mol. Catal.* **1983**, *21*, 297.
(15) Jensen, C. M.; Chen, Y. J.; Kaesz, H. D. *J. Am. Chem. Soc.* **1984**, *106*, 4046.
(16) Collman, J. P.; Hegedus, L. S.; Norton, J. R.; Finke, R. G. *Principles and Applications of Organotransition Metal Chemistry*; University Science Books: Mill Valley, CA, 1987.
(17) Semmelhack, M. F.; Tamura, R. *J. Am. Chem. Soc.* **1983**, *105*, 4099.
(18) Aitchison, A. A.; Farrugia, L. *J. Organometallics* **1986**, *5*, 1103 and references cites therein.
(19) (a) LaCroce, S. J.; Menard, K. P.; Cutler, A. R. *J. Organomet. Chem.* **1980**, *190*, C79. (b) Fong, R. H.; Hersh, W. H. *Organometallics* **1985**, *4*, 1468.
(20) Ros, J.; Commenges, G.; Mathieu, R.; Solans, X.; Font-Altaba, M. *J. Chem. Soc., Dalton Trans.* **1985**, 1087.
(21) Finke, R. G.; Gaughan, G.; Pierpont, C.; Noordik, J. H. *Organometallics* **1983**, *2*, 1481 and references cited therein.
(22) Krause, M. J.; Bergman, R. G. *Organometallics* **1986**, *5*, 2097.
(23) Schore, N. E.; Ilenda, C. S.; White, M. A.; Bryndza, H. E.; Matturro, M. G.; Bergman, R. G. *J. Am. Chem. Soc.* **1984**, *106*, 7451.
(24) Available at: Project SERAPHIM, NSF Science Education Project, Department of Chemistry, University of Wisconsin, 1101 University Ave., Madison, WI 53706.

probability at the metal or at the oxygen of the bridging carbonyl ligand. Oxygen protonation is a much rarer event even with carbonyl clusters where the metal hydride is the more stable product. In previous studies of $Ru_2(dmpm)_2(CO)_5$ we reported that protonation occurs with high yield at the Ru–Ru bond, leading to structure **7**.[2]

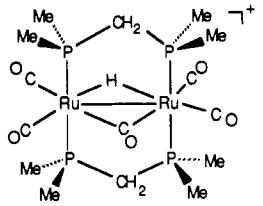

7

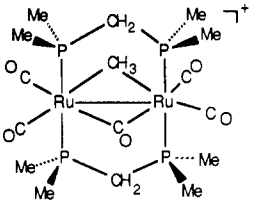

8

Because of the anticipated instability of a bridging methyl group relative to that of a terminal methyl, isolation of the analogous product (**8**) resulting from the methylation of the Ru–Ru bond would be unexpected. However, the most sterically accessible and electron-rich site on the dimer is the Ru–Ru bond. We propose that methylation, at least with methyl triflate, does occur on the metal–metal bond but that this rapidly rearranges through **2** to the more stable complex **3**.

Studies of the solutions of **4** show that it does not convert to **3**, and likewise, once **3** is formed, the only subsequent reaction is conversion to the terminal (**5**) and bridging (**6**) acetyl complexes. This suggests that k_1 and k_2 in Scheme I are both irreversible. The surprising observation that the yields of the two products are the same at all temperatures studied further suggests that $k_1 = k_2$. We conclude that the nature of the product depends simply on the side of the complex that is presented to the electrophile as the bond is being formed.

Once formed, **3** reacts rapidly with CO to form two complexes containing an acyl ligand. Unfortunately, the facile equilibrium between the terminal (**5**) and bridging (**6**) acyl complexes precludes any conclusion being drawn regarding the order of their formation from the alkyl complex.

Summary

The methylation of $Ru_2(dmpm)_2(CO)_5$ was found to result in equal amounts of metal- and oxygen-methylated products. The structure of the O-methylated product was determined by X-ray diffraction and is the first structurally characterized example of a bimetallic complex containing a μ-alkoxymethylidyne ligand. The Ru-methylated product was found to react with CO to form the η^1-acetyl species $[Ru_2(dmpm)_2(CO)_5[C(O)CH_3]]^+$. This complex loses CO at room temperature, resulting in formation of the μ-acetyl species $[Ru_2(dmpm)_2(CO)_4[\mu\text{-}C(O)CH_3]]^+$. $[Ru_2(dmpm)_2(CO)_5[C(O)CH_3]]^+$ and $[Ru_2(dmpm)_2(CO)_4[\mu\text{-}C(O)CH_3]]^+$ were shown to be interconvertible at room temperature. Additional studies of the reactivity of $Ru_2(dmpm)_2(CO)_5$ are in progress.

Acknowledgment. This research was supported by a grant from the National Science Foundation (Grant No. CHE-8714326).

Registry No. 1, 123810-59-3; [3][CF_3SO_3], 127356-70-1; [4][CF_3SO_3], 127356-72-3; [5][CF_3SO_3], 127356-74-5; [6][CF_3SO_3], 127356-76-7; $CF_3SO_3CH_3$, 333-27-7.

Supplementary Material Available: Listings of hydrogen atom positions, anisotropic temperature factors, and non-hydrogen bond distances and angles (7 pages); a listing of structure factors (27 pages). Ordering information is given on any current masthead page.

Decomposition Kinetics of 1,1,2- and 1,1,1-Trimethyldisilane

K. E. Nares, G. F. Licciardi, H. E. O'Neal,* and M. A. Ring*

Department of Chemistry, San Diego State University, San Diego, California 92182

Received January 18, 1990

The thermal decomposition kinetics of the titled disilanes obtained from static system investigations under conditions of maximum quenching of silylene chains are reported. Single-pulse shock-tube kinetic results on the 1,1,2-trimethyldisilane decomposition as well as relative rate kinetics of silylene insertions into silane and methylsilane at elevated temperatures are also given. Comparisons of the latter with room-temperature absolute rate constants support the consecutive-step, double-transition-state hypothesis for these reactions.

Introduction

It is now known[1] that the only important primary dissociation reactions (PDR's) of disilanes containing Si–H bonds are 1,2-H-shift silylene eliminations, as illustrated for 1,1-dimethyldisilane:

$$Me_2SiHSiH_3 \rightarrow Me_2SiH_2 + SiH_2 \quad (1)$$
$$\rightarrow SiH_4 + Me_2Si \quad (2)$$

It has also been established that disilane decompositions leading to the same products can be induced by silylene chain processes.[2] Thus, in the neat 1,1-dimethyldisilane decomposition eqs 3–5 are very important and eq 4 is the main source of silane.

$$SiH_2 + Me_2SiHSiH_3 \rightleftharpoons Me_2SiHSiH_2SiH_3 \quad (3)$$
$$Me_2SiHSiH_2SiH_3 \rightleftharpoons Me_2SiHSiH + SiH_4 \quad (4)$$
$$\rightleftharpoons Me_2SiH_2 + SiHSiH_3 \quad (5)$$

Such chains can be difficult to quench. In the above system, complete quenching was not achieved even with

(1) (a) Estacio, P.; Sefcik, M. D.; Chan, E. K.; Ring, M. A. *Inorg. Chem.* **1970**, *9*, 1068. (b) Baird, R. B.; Sefcik, M. D.; Ring, M. A. *Inorg. Chem.* **1971**, *10*, 883. (c) Bowrey, M.; Purnell, J. H. *J. Am. Chem. Soc.* **1970**, *92*, 2594. (d) Vanderwielen, A. J.; Ring, M. A.; O'Neal, H. E. *J. Am. Chem. Soc.* **1975**, *97*, 993.

(2) Nares, K. E.; Harris, M. E.; Ring, M. A.; O'Neal, H. E. *Organometallics* **1989**, *8*, 1964.

0276-7333/90/2309-2105$02.50/0